

Development of Tunnel Magneto-Resistive Sensors

Mikihiko OOGANE^{†a)}, Nonmember

SUMMARY The magnetic field resolution of the tunnel magneto-resistive (TMR) sensors has been improving and it reaches below $1.0 \text{ pT/Hz}^{0.5}$ at low frequency. The real-time measurement of the magnetocardiography (MCG) and the measurement of the magnetoencephalography (MEG) have been demonstrated by developed TMR sensors. Although the MCG and MEG have been applied to diagnosis of diseases, the conventional MCG/MEG system using superconducting quantum interference devices (SQUIDs) cannot measure the signal by touching the body, the body must be fixed, and maintenance costs are huge. The MCG/MEG system with TMR sensors operating at room temperature have the potential to solve these problems. In addition, it has the great advantage that it does not require a special magnetic shielded room. Further developments are expected to progress to maximize these unique features of TMR sensors.

key words: Spintronics, magnetic tunnel junctions (MTJs), tunnel magneto-resistive sensor (TMR sensor), bio-magnetic field

1. Introduction

After the theoretical prediction of a large tunnel magnetoresistance (TMR) effect in magnetic tunnel junctions (MTJs) with Fe/MgO/Fe structure [1], [2], S. Yuasa *et al.* experimentally demonstrated 88% TMR effect at room temperature in an epitaxially grown Fe(001)/MgO(001)/Fe(001)-MTJs prepared by the molecular beam epitaxy (MBE) method [3]. Subsequently, S. Yuasa *et al.* and S. S. Parkin *et al.* successfully observed a very large TMR ratio of ca. 200% at RT in MTJs with an MgO tunneling barrier layer [4], [5]. Furthermore, D. Djayaprawira *et al.* developed MTJs with CoFeB/MgO/CoFeB structure on a Si substrate and achieved a large TMR ratio of 230% at RT [6]. In these practical MTJs, the CoFeB electrodes are crystallized into CoFe after the annealing process. A large TMR ratio can be observed even in CoFeB/MgO/CoFeB-MTJs as same as the Fe/MgO/Fe structure due to the crystallization of CoFeB layers.

Because of the large TMR effect in CoFeB/MgO/CoFeB based-MTJs, these MTJs can be applied to the magnetic-random-access memory (MRAM) and the highly sensitive magnetic sensor (TMR sensor). Figure 1 shows a schematic image of magnetoresistance curves for MRAMs and TMR sensors. A binary state of high and low resistance is need for MRAMs. On the other hand, it is required that the resistance changes linearly around the low magnetic field for TMR sensors. Although hard ferromagnetic materials are

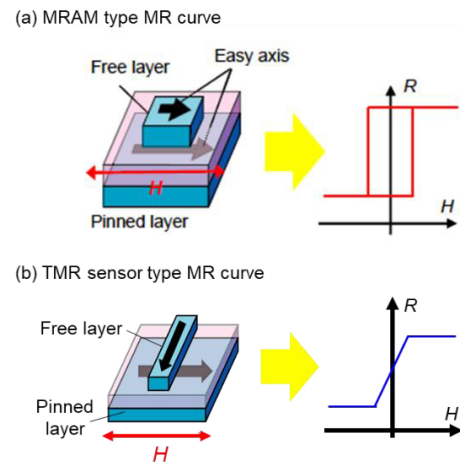


Fig. 1 Magneto-resistive curves for (a) MRAMs and (b) TMR sensors

needed to keep the memory in MRAMs, very soft ferromagnetic materials are used to achieve a high sensitivity in TMR sensors. Recently, the CoFeB/MgO/CoFeB based-MTJs with both a high TMR effect and very soft magnetic properties of the ferromagnetic layer have been developed. Utilizing such highly-sensitive TMR sensors, the detection of a weak magnetic field such as a bio-magnetic field has been demonstrated at room temperature [7]–[9].

The TMR sensors can operate at room temperature, and both their device size and power consumption are small because the MTJ device has a relatively large resistance. Furthermore, TMR sensors can be prepared on large Si wafers using a micro-fabrication technique. Because of these features, TMR sensors can be widely used not only for the bio-magnetic field detection. Researches on non-destructive inspection for infrastructures, electric current monitoring for EV batteries using TMR sensors have been carried out [10], [11]. In this invited paper, the operation principle of TMR sensors, recent progress on the TMR sensor development (improvement of the sensitivity and reduction in $1/f$ noise in TMR sensors), and a bio-magnetic field measurement using TMR sensors are described.

2. Operation Principle of TMR Sensors

The linear output against the external magnetic field for the TMR sensors is explained by the Stoner-Wohlfarth model that the magnetization coherently rotates in the ferromagnetic material with uniaxial magnetic anisotropy [12]. The

Manuscript received July 23, 2023.

Manuscript revised October 10, 2023.

Manuscript publicized December 4, 2023.

[†]The author is with Tohoku University, Sendai-shi, 980–8579 Japan.

a) E-mail: mikihiko.ogane.e4@tohoku.ac.jp

DOI: 10.1587/transle.2023SEI0001

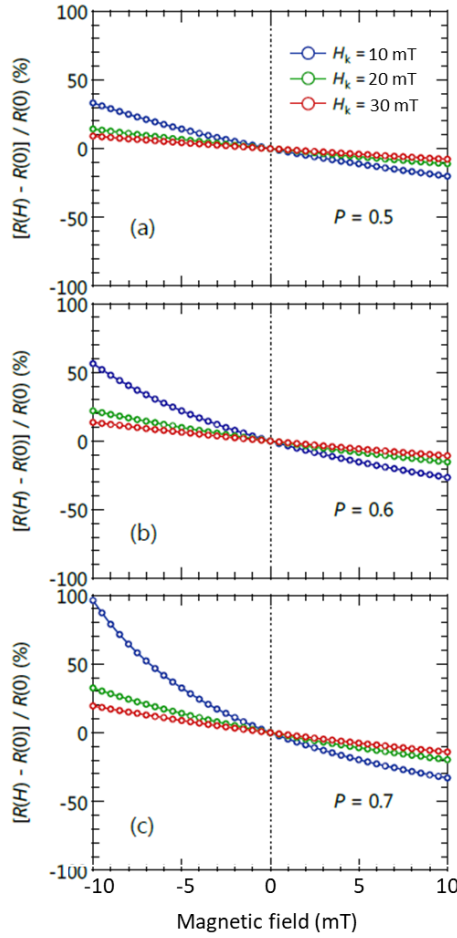


Fig. 2 Calculated $R - H$ curves with (a) $P = 0.5$, (b) $P = 0.6$, and (c) $P = 0.7$. H_k for red, blue, and green lines are 10, 20, and 30 mT respectively

total energy E in the ferromagnetic materials with uniaxial magnetic anisotropy energy (K_u) is expressed as follows.

$$E = -M_s H \cos \theta - K_u \cos^2(\theta_0 - \theta) \quad (1)$$

Here, the first term is magneto-static energy. The saturated magnetization M_s makes an angle θ with magnetic field H . The second term is magnetic anisotropic energy. The external magnetic field makes an angle θ_0 with magnetic easy axis. An angle θ is determined by the minimum energy condition of $dE/d\theta = 0$. When H is applied along the hard-axis direction, $\theta_0 = \pi/2$, the magnetization M ($= M_s \cos \theta$) is expressed as follows.

$$M = M_s^2 H / 2K_u \quad (2)$$

Therefore, M proportionally increases with H and saturates at magnetic anisotropy field $H_k = 2K_u/M_s$.

On the other hand, the tunneling conductance in the MTJs is expressed by the following equation according to the Slonczewski's model [13].

$$G = G_0(1 + P^2 \cos \theta) \quad (3)$$

Here, θ is the relative angle of the two ferromagnetic layers in

MTJs, G_0 is the conductance at zero magnetic field, and P is the tunneling spin polarization for the ferromagnetic layers. When the magnetization of the pinned layer is completely fixed against the external magnetic field, θ is determined by the magnetization direction of the free layer in MTJs. From the Eqs. (2) and (3), the tunneling conductance is expressed as follows when magnetic field H is applied along the hard-axis direction of the free layer.

$$G = G_0(1 + P^2 H/H_k) \quad (4)$$

From the Eq. (4), it is obvious that the tunneling conductance is proportional to the external magnetic field H , and its slope is determined by the square of the spin polarization P and the magnetic anisotropy field H_k . Therefore, the large spin polarization (the large TMR ratio) and small magnetic anisotropy field are needed to enhance the sensitivity in the TMR sensors. Figure 2 shows calculated $R - H$ curves using Eq. (4) with various P and H_k . Note that the $R - H$ curves are linear when the external magnetic field is sufficiently smaller than H_k , however, the nonlinearity increases as the external magnetic field approaches H_k . Furthermore, the slope of $R - H$ curves increases as the spin polarization P increases, but the nonlinearity also increases. Therefore, the magnitude of H_k needs to be sufficiently large with respect to the measured bio-magnetic field to obtain a linear output of the TMR sensors.

3. Improvement of the Sensitivity in TMR Sensors

A very large sensitivity is required to measure a weak magnetic field, such as bio-magnetic field of pico-Tesla. At least, a high sensitivity above 100%/mT is needed for bio-magnetic field measurement to obtain the output voltage of nV for TMR sensors with 100×100 MTJ arrays [14]. Here, the sensitivity of TMR sensors is defined as $\text{TMR}/2H_k$, where H_k is a magnetic anisotropy field of the free layer. TMR ratio has been improved by development of the ferro magnetic materials [15]–[18] and optimization of the fabrication condition and the stacking structure in MTJs [19], [20]. On the other hand, the reduction in magnetic anisotropy field H_k has been achieved by magnetic flux concentrators (MFCs) [21]–[24], and utilizing soft ferromagnetic materials [25], [26].

In our previous study, in order to realize both a high TMR ratio and small H_k , an anti-ferromagnetic coupled NiFe/Ru/CoFeB free layers have been developed [25]. The typical structure of sensor-type MTJs with an anti-ferro coupled free layer is shown in Fig. 3 (a). For the anti-ferromagnetic coupled free layer, the magnetization of the NiFe and CoFeB layers are magnetically coupled through the thin Ru layer by the RKKY-type interaction. When the thickness of NiFe layer is thick compared with CoFeB, the magnetization of the CoFeB follows the magnetization rotation of the NiFe. As a result, a small H_k can be realized by soft-magnetic property of NiFe layer and a high TMR can be obtained by the CoFeB layer at the MgO barrier interface.

Figure 3 (b) shows a magneto-resistive (MR) curve around zero fields for the MTJs with NiFe/Ru/CoFeB free

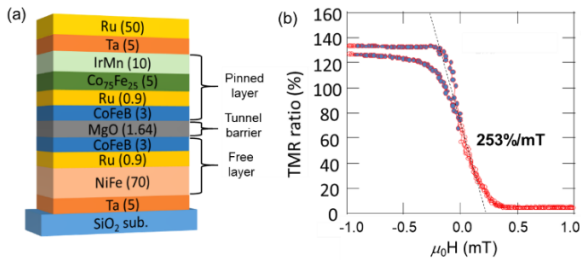


Fig. 3 (a) Typical film structure and (b) MR curve for MTJs with NiFe/Ru/CoFeB free layer

layer. By optimization of the NiFe thickness and the condition of the magnetic annealing process, the linear output with small hysteresis was obtained, and a very high sensitivity of 253%/mT was successfully observed [25].

Although the relatively high sensitivity of ca. 250%/mT was achieved in the MTJs with NiFe/Ru/CoFeB free layer, TMR ratio was limited below 200%, because the NiFe has fcc-structure which is not compatible with the NaCl structure of MgO barriers. In order to enhance the TMR effect, the Co-based amorphous material, CoFeSiB, was used as a free layer of MTJs instead of the NiFe. The Co-based amorphous also shows a good soft-magnetic property and the MTJs with CoFeSiB/Ru/CoFeB free layer showed a very high sensitivity of 1,150%/mT [8]. This is the highest sensitivity in the TMR sensors without the MFCs up to now.

4. Reduction in the $1/f$ Noise in TMR Sensors

There are some methods for reducing $1/f$ noise in TMR sensors. One is a method to avoid $1/f$ noise by modulating the frequency into the high frequency utilizing the chopping technique and the MEMS. By the high frequency modulation, the noise reduction in MTJs was demonstrated [27], [28]. Additionally, a weak magnetic field of pico-Tesla was detected by combination with these techniques [29].

Another method for reduction in $1/f$ noise is an integration of MTJs connected in series and/or parallel [14]. In our previous study, an MTJ array with 100×100 MTJs was developed to reduce $1/f$ noise [30]. Figure 4 shows the noise power spectrum density (S_V^2) of the single MTJ and 100×100 integrated MTJs at bias voltage of 30 mV in a parallel magnetization state. The stacking structure of MTJs was same as seen in Fig. 3 (a). As shown in Fig. 4, $1/f$ noise dominated the low-frequency region and the noise for the 100×100 integrated MTJs was much smaller than that for the single MTJ. This result indicates that the integration of MTJs is greatly useful to reduce $1/f$ noise in TMR sensors.

In addition, the reduction of electrical $1/f$ noise was demonstrated by the decrease in the MgO barrier thickness [8]. Since one of the origins of the electrical $1/f$ noise is hopping tunneling through the defects in the MgO barriers, the reduction in MgO barrier thickness is effective to reduce the hopping states and the electrical $1/f$ noise.

Since the sensitivity and $1/f$ noise in TMR sensors have been improved, the magnetic field resolution of the TMR

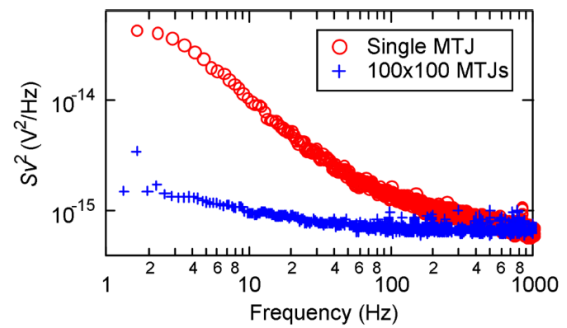


Fig. 4 Noise power density in 100×100 MTJ array and single MTJ

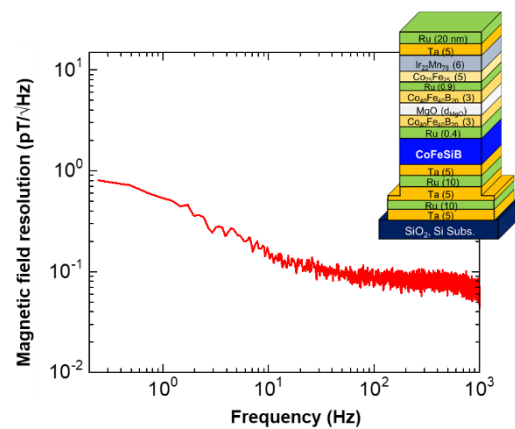


Fig. 5 Frequency dependence of magnetic field resolution in TMR sensor

sensors at low frequency has been dramatically improved. Figure 5 shows the frequency dependence of the magnetic field resolution in the typical developed TMR sensor. The free layer structure of the MTJs was CoFeSiB/Ru/CoFeB to obtain both high TMR and low H_k as mentioned above. The TMR sensor has a structure in which 74 MTJs with device area of $50 \times 50 \mu\text{m}^2$ are connected in series to reduce the $1/f$ noise. In addition, on both sides of the MTJ arrays, T-shaped magnetic flux concentrators (MFCs) to concentrate the external magnetic field were attached. The T-shaped MFCs has a size of 12.5 mm in the direction of the sensing axis (vertical line of “T”) and 26.0 mm in the direction parallel to the MTJ array (horizontal line of “T”). The gain of T-shaped MFCs was about 70 at 1 Hz. The detailed device structure and properties of TMR sensors was described in our previously reported paper [8]. As shown in Fig. 5, a very small magnetic field resolution of $0.5 \text{ pT/Hz}^{0.5}$ was achieved at 1 Hz. This is the minimum magnetic field resolution in TMR sensors at low frequency. In addition, the magnetic field resolution reached to ca. $60 \text{ fT/Hz}^{0.5}$ at 1 kHz. The proton-NMR measurement under low dc-field of $50 \mu\text{T}$ was demonstrated thanks to the small magnetic field resolution at kHz region [8]. The obtained performance at room temperature for developed TMR sensors is close to SQUID devices.

5. Bio-Magnetic Field Measurement by TMR Sensors

The TMR sensor module for magnetocardiography (MCG) measurement was developed. For the MCG module, a TMR sensor was used as one of the resistors in the full-bridge circuit, and its output voltage was amplified and filtered. Bias voltage of ± 0.2 V was supplied to the bridge circuit. MCG signals measured by the TMR sensor bridge were amplified by two-stage amplification circuit with a total gain of 100 dB (60 + 40 dB). The sensitivity of the fabricated sensor system was 0.33 V/nT. In addition, the signals were shaped by an analog bandpass filter from 0.1 to 50 Hz. Figure 6 shows the typical result of a real-time MCG measurement in the magnetic shielded room. The TMR sensor module was placed several millimeters away from the body surface and detected the transverse component of the magnetic field. As shown in Fig. 6, a clear R-peak was observed without signal averaging. The amplitude of the transverse magnetic field related to the R-peaks was approximately 200–300 pT, which is consistent with the reported value measured by SQUIDs. Furthermore, we have recently demonstrated magnetic shield room less MCG measurement using 96-channel 3-axes TMR sensors and an environmental noise cancelling technique [31].

The measurement system for magnetoencephalography (MEG) using TMR sensors was also developed. A TMR sensor was used as one of the resistors in the bridge circuit, and its output voltage was amplified and filtered. The bridge was supplied with ± 0.2 V as same as the MCG measurement. The circuit to receive the signal from the bridge was

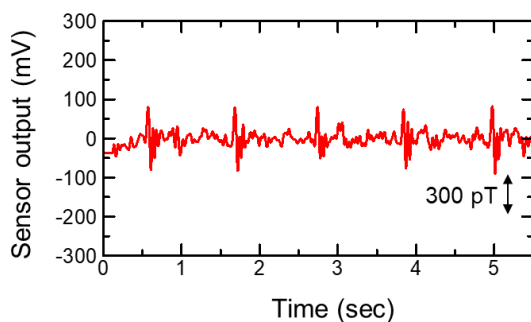


Fig. 6 Real-time MCG measurement result by TMR sensor module

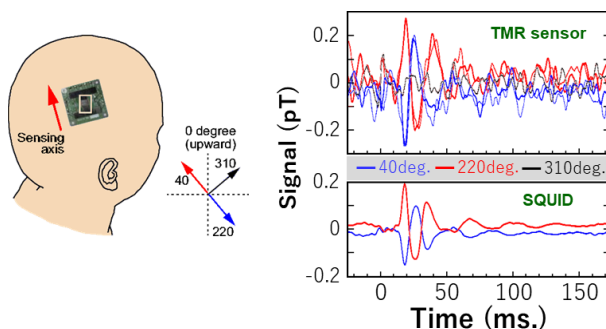


Fig. 7 MEG measurement results by TMR sensor and SQUID-MEG

constructed by ourselves using instrumentation amplifiers and CR passive filters. The MEG signal measured by the TMR sensor was input to a two-stage amplification circuit with a total gain of 120 dB (60 + 60 dB), and was shaped by an analog bandpass filter from 0.08 Hz to 2 kHz. The signal output of the fabricated sensor system was 2.36 V/nT, and the magnetic field resolution measured in a magnetic shielded room was 0.9 pT/Hz^{0.5} at 10 Hz. The amplified and filtered signals were recorded on a PC at sampling rate of 2 kHz using an "AD Instruments PowerLab 16/35" and "LabChart8" software. The MEG signals were filtered in the software with a moving average (digital filter) from 20 Hz to 200 Hz. The pulse signal of the stimulation was also measured using the analog-to-digital converter at the same time, and the MEG signal was integrated 5,000 times by using the rising edge of the pulse as a trigger.

The somatosensory evoked fields (SEFs) were measured for the left median nerve stimuli using a developed measurement system. First, the N20m source position and orientation were estimated using SQUID-MEG system in the magnetic shielded room. Then, a TMR sensor bridge was placed on the right parietal scalp directly to measure tangential component of MEG as shown in Fig. 7. Sensing axis of the sensor was set at 40, 220 and 310 degrees from the upward direction of the subject. The peaks of N20m and the following P30m components of SEF were clearly measured as shown in Fig. 7. We confirmed that the observed signals were almost identical to radial components measurement by SQUID-MEG system [9]. Further improvement of the sensitivity in TMR sensors will realize a high-spatial resolution of MEG mapping and a short measurement time in the future.

Acknowledgments

This work was supported by the Center for Science and Innovation in Spintronics (CSIS) and the Center for Innovative Integrated Electronic System (CIES) in Tohoku University and the NEDO leading program, the SIP project, and X-nics project.

References

- [1] W.H. Butler, X.-G. Zhang, T.C. Schulthess, and J.M. MacLaren, "Spin-dependent tunneling conductance of Fe|MgO|Fe sandwiches," *Phys. Rev. B*, vol.63, no.5, p.054416, 2001.
- [2] J. Mathon and A. Umerski, "Theory of tunneling magnetoresistance of an epitaxial Fe/MgO/Fe(001) junction," *Phys. Rev. B*, vol.63, no.22, p.220403, 2001.
- [3] S. Yuasa, A. Fukushima, T. Nagahama, K. Ando, and Y. Suzuki, "High Tunnel Magnetoresistance at Room Temperature in Fully Epitaxial Fe/MgO/Fe Tunnel Junctions due to Coherent Spin-Polarized Tunneling," *Jpn. J. Appl. Phys.*, vol.43, no.4B, p.L588, 2004.
- [4] S. Yuasa, T. Nagahama, A. Fukushima, Y. Suzuki, and K. Ando, "Giant room-temperature magnetoresistance in single-crystal Fe/MgO/Fe magnetic tunnel junctions," *Nat. Mater.*, vol.3, no.12, pp.868–871, 2004.
- [5] S.S.P. Parkin, C. Kaiser, A. Panchula, P.M. Rice, B. Hughes, M. Samant, and S.-H. Yang, "Giant tunnelling magnetoresistance at room temperature with MgO (100) tunnel barriers," *Nat. Mater.*, vol.3, no.12, pp.862–867, 2004.

- [6] D.D. Djayaprawira, K. Tsunekawa, M. Nagai, H. Maehara, S. Yamagata, N. Watanabe, S. Yuasa, Y. Suzuki, and K. Ando, "230% room-temperature magneto-resistance in CoFeB/MgO/CoFeB magnetic tunnel junctions," *Appl. Phys. Lett.*, vol.86, no.9, p.092502, 2005.
- [7] K. Fujiwara, M. Oogane, A. Kanno, M. Imada, J. Jono, T. Terauchi, T. Okuno, Y. Aritomi, M. Morikawa, M. Tsuchida, N. Nakasato, and Y. Ando, "Magneto-cardiography and magneto-encephalography measurements at room temperature using tunnel magneto-resistance sensors," *Applied Physics Express*, vol.11, no.2, p.023001, 2018.
- [8] M. Oogane, K. Fujiwara, A. Kanno, T. Nakano, H. Wagatsuma, T. Arimoto, S. Mizukami, S. Kumagai, H. Matsuzaki, N. Nakasato, and Y. Ando, "Sub-pT magnetic field detection by tunnel magneto-resistive sensors," *Appl. Phys. Express*, vol.14, no.12, p.123002, 2021.
- [9] A. Kanno, N. Nakasato, M. Oogane, K. Fujiwara, T. Nakano, T. Arimoto, H. Matsuzaki, and Y. Ando, "Scalp attached tangential magnetoencephalography using tunnel magneto-resistive sensors," *Scientific Reports*, vol.12, 6106, 2022.
- [10] Z. Jin, M.A.I. Mohd Noor Sam, M. Oogane, and Y. Ando, "Serial MTJ-based TMR sensors in bridge configuration for detection of fractured steel bar in magnetic flux leakage testing," *Sensors*, vol.21, no.2, p.668, 2021.
- [11] T. Ogasawara, M. Oogane, M. Al-Mahdawi, M. Tsunoda, and Y. Ando, "Effect of second-order magnetic anisotropy on nonlinearity of conductance in CoFeB/MgO/CoFeB magnetic tunnel junction for magnetic sensor devices," *Scientific Reports*, vol.9, no.1, p.17018, 2019.
- [12] E.C. Stoner and E.P. Wohlfarth, "A mechanism of magnetic hysteresis in heterogeneous alloys," *Philos. Trans. R. Soc. A*, vol.240, 599, 1948.
- [13] J.C. Slonczewski, "Conductance and exchange coupling of two ferromagnets separated by a tunneling barrier," *Phys. Rev. B*, vol.39, no.10, pp.6995–7002, 1989.
- [14] M. Tondra et al., "Picotesla field sensor design using spin-dependent tunneling devices," *J. Appl. Phys.*, vol.83, no.11, pp.6688–6690, 1998.
- [15] S. Yuasa, A. Fukushima, H. Kubota, Y. Suzuki, and K. Ando, "Giant tunneling magnetoresistance up to 410% at room temperature in fully epitaxial Co/MgO/Co magnetic tunnel junctions with bcc Co(001) electrodes," *Appl. Phys. Lett.*, vol.89, no.4, p.042505, 2006.
- [16] S. Tsunegi, Y. Sakuraba, M. Oogane, K. Takanashi, and Y. Ando, "Large tunnel magnetoresistance in magnetic tunnel junctions using a Co₂MnSi Heusler alloy electrode and a MgO barrier," *Appl. Phys. Lett.*, vol.93, no.11, p.112506, 2008.
- [17] N. Tezuka, N. Ikeda, F. Mitsuhashi, and S. Sugimoto, "Improved tunnel magnetoresistance of magnetic tunnel junctions with Heusler Co₂FeAl_{0.5}Si_{0.5} electrodes fabricated by molecular beam epitaxy," *Appl. Phys. Lett.*, vol.94, no.16, p.162504, 2009.
- [18] H. Sukegawa, Y. Miura, S. Muramoto, S. Mitani, T. Niizeki, T. Ohkubo, K. Abe, M. Shirai, K. Inomata, and K. Hono, "Enhanced tunnel magnetoresistance in a spinel oxide barrier with cation-site disorder," *Phys. Rev. B*, vol.86, no.18, p.184401, 2012.
- [19] Y.M. Lee, J. Hayakawa, S. Ikeda, F. Matsukura, and H. Ohno, "Effect of electrode composition on the tunnel magnetoresistance of pseudo-spin-valve magnetic tunnel junction with a MgO tunnel barrier," *Appl. Phys. Lett.*, vol.90, no.21, p.212507, 2007.
- [20] S. Ikeda, J. Hayakawa, Y. Ashizawa, Y.M. Lee, K. Miura, H. Hasegawa, M. Tsunoda, F. Matsukura, and H. Ohno, "Tunnel magnetoresistance of 604% at 300K by suppression of Ta diffusion in CoFeB/MgO/CoFeB pseudo-spin-valves annealed at high temperature," *Appl. Phys. Lett.*, vol.93, no.8, p.082508, 2008.
- [21] J.P. Valadeiro, J. Amaral, D.C. Leitao, R. Ferreira, S.F. Cardoso, and P.J.P. Freitas, "Strategies for pTesla Field Detection Using Magnetoresistive Sensors With a Soft Pinned Sensing Layer," *IEEE Trans. Magn.*, vol.51, no.1, 4400204, 2015.
- [22] R.C. Chaves, P.P. Freitas, B. Ocker, and W. Maass, "MgO based picotesla field sensors," *J. Appl. Phys.*, vol.103, no.7, p.07E931, 2008.
- [23] S. Cardoso, D.C. Leitao, L. Gameiro, F. Cardoso, R. Ferreira, E. Paz, and P.P. Freitas, "Magnetic tunnel junction sensors with pTesla sensitivity," *Microsyst. Technol.*, vol.20, no.4-5, pp.793–802, 2014.
- [24] R.C. Chaves, P.P. Freitas, B. Ocker, and W. Maass, "Low frequency picotesla field detection using hybrid MgO based tunnel sensors," *Appl. Phys. Lett.*, vol.91, no.10, p.102504, 2007.
- [25] K. Fujiwara, M. Oogane, S. Yokota, T. Nishikawa, H. Naganuma, and Y. Ando, "Fabrication of magnetic tunnel junctions with a bottom synthetic antiferro-coupled free layers for high sensitive magnetic field sensor devices," *J. Appl. Phys.*, vol.111, no.7, p.07C710, 2012.
- [26] D. Kato, M. Oogane, K. Fujiwara, T. Nishikawa, H. Naganuma, and Y. Ando, "Fabrication of Magnetic Tunnel Junctions with Amorphous CoFeSiB Ferromagnetic Electrode for Magnetic Field Sensor Devices," *Appl. Phys. Express*, vol.6, no.10, p.103004, 2013.
- [27] A. Jander, C.A. Nordman, A.V. Pohm, and J.M. Anderson, "Chopping techniques for low-frequency nanotesla spin-dependent tunneling field sensors," *J. Appl. Phys.*, vol.93, no.10, pp.8382–8384, 2003.
- [28] A.S. Edelstein, G.A. Fischer, M. Pedersen, E.R. Nowak, S.F. Cheng, and C.A. Nordman, "Progress toward a thousand fold reduction in 1/f noise in magnetic sensors using an ac microelectromechanical system flux concentrator," *J. Appl. Phys.*, vol.99, no.8, p.08B317, 2006.
- [29] W.F. Egelhoff Jr., P.W.T. Pong, J. Unguris, R.D. McMichael, E.R. Nowak, A.S. Edelstein, J.E. Burnette, and G.A. Fischer, "Critical Challenges for Picotesla Magnetic- Tunnel-Junction Sensors," *Sensors and Actuators A*, vol.155, no.2, pp.217–225, 2009.
- [30] K. Fujiwara, M. Oogane, T. Nishikawa, H. Naganuma, and Y. Ando, "Detection of Sub-Nano-Tesla Magnetic Field by Integrated Magnetic Tunnel Junctions with Bottom Synthetic Antiferro-Coupled Free Layer," *Jpn. J. Appl. Phys.*, vol.52, no.4S, p.04CM07, 2013.
- [31] K. Kurashima, M. Kataoka, T. Nakano, K. Fujiwara, S. Kato, T. Nakamura, M. Yuzawa, M. Masuda, K. Ichimura, S. Okatake, Y. Moriyasu, K. Sugiyama, M. Oogane, Y. Ando, S. Kumagai, H. Matsuzaki, and H. Mochizuki, "Development of Magnetocardiograph without Magnetically Shielded Room Using High-Detectivity TMR Sensors," *Sensors*, vol.23, no.2, p.646, 2023.



Mikihiko Oogane received Ph.D. degree in the Department of Applied Physics from Tohoku University, Japan, in 2003. Since 2022, he has been a Professor with the Department of Applied Physics, Tohoku University, Japan. He is the author of more than 200 articles. His research interest includes the development of spintronic materials and devices. In particular, he has made remarkable achievements in the development and application of magnetic tunnel junction devices. Dr. Mikihiko Oogane was a recipient of the Magnetics Society of Japan Young Researcher Award for Excellence in 2007 and JSAP Outstanding Paper Award in 2022.